Analytical Methods

ROYAL SOCIETY OF CHEMISTRY

PAPER

View Article Online
View Journal | View Issue

Check for updates

Cite this: *Anal. Methods*, 2024, **16**, 1074

Open Access Article. Published on 29 January 2024. Downloaded on 5/21/2024 3:39:05 PM.
This article is licensed under a Creative Commons Attribution 3.0 Unported Licence.

Analysis of tryptophan metabolites and related compounds in human and murine tissue: development and validation of a quantitative and semi-quantitative method using high resolution mass spectrometry†

Sandy Abujrais, [ab] S. J. Kumari A. Ubhayasekera [ab] and Jonas Bergquist *[ab]

This study explores the metabolic differences between human and murine plasma in addition to differences between murine subcutaneous and visceral white adipose tissue. A quantitative and semi-quantitative targeted method was developed and validated for this purpose. The quantitative method includes tryptophan and its metabolites in addition to tyrosine, phenylalanine, taurine, B vitamins, neopterin, cystathionine and hypoxanthine. While the semi-quantitative method includes; 3-indoleacetic acid, 5-hydroxyindoleacetic acid, acetylcholine, asymmetric dimethylarginine, citrulline and methionine. Sample preparation was based on protein precipitation, while quantification was conducted using ultrahigh-performance liquid chromatography coupled to a quadrupole Orbitrap tandem mass spectrometer with electrospray ionization in the parallel reaction monitoring (PRM) mode. The low limit of quantification for all metabolites ranged from 1 to 200 ng mL^{-1}. Matrix effects and recoveries for stable isotope labelled internal standards were evaluated, with most having a coefficient of variation (CV) of less than 15%. Results showed that a majority of the analytes passed both the intra- and interday precision and accuracy criteria. The comparative analysis of human and murine plasma metabolites reveals species-specific variations within the tryptophan metabolic pathway. Notably, murine plasma generally exhibits elevated concentrations of most compounds in this pathway, with the exceptions of kynurenine and quinolinic acid. Moreover, the investigation uncovers noteworthy metabolic disparities between murine visceral and subcutaneous white adipose tissues, with the subcutaneous tissue demonstrating significantly higher concentrations of tryptophan, phenylalanine, tyrosine, and serotonin. The findings also show that even a semi-quantitative method can provide comparable results to quantitative methods from other studies and be effective for assessing metabolites in a complex sample. Overall, this study provides a robust platform to compare human and murine metabolism, providing a valuable insight to future investigations.

Received 5th November 2023
Accepted 22nd January 2024

DOI: 10.1039/d3ay01959d

rsc.li/methods

1 Introduction

Tryptophan (Trp) is an essential amino acid and has distinctive molecular properties. It is the only amino acid with two rings in its side-chain.[1] Trp is degraded into three major pathways; the kynurenine, serotonin and indole as illustrated in the ESI Fig. S1.†[2] In humans, kynurenine is primarily synthesized endogenously from tryptophan. The liver is primarily responsible for the production of kynurenine under physiological conditions through tryptophan 2,3-dioxygenase (TDO) enzyme, which is primarily expressed in the liver. TDO can also be present in other cell types like neurons.[3–5] Additionally, a smaller portion of kynurenine is produced by indole amine dioxygenase (IDO) enzyme, which is present in various parts of the body.[6] Increasing levels of inflammatory signals, such as interleukins, can activate the IDO enzyme, whereas stress hormones like cortisol can activate the TDO enzyme.[7] Kynurenine levels are thus affected by our dietary intake of tryptophan, TDO and IDO activity, stress hormones and inflammatory signals. Kynurenine has two main pathways: *i.e.* to form kynurenic acid by the enzyme kynurenine aminotransferase (KAT) or to form 3-hydroxyanthranilic acid by kynureninase and or/kynurenine 3-monooxygenase (KMO).[8] The kynurenine pathway plays a critical role in the development of neurological disorders, including Alzheimer's disease,[9] Parkinson's disease[10] and major depression,[11] as it affects the nervous system and

[a]*Analytical Chemistry and Neurochemistry, Department of Chemistry – BMC, Uppsala University, Box 599, 75124, Uppsala, Sweden. E-mail: jonas.bergquist@kemi.uu.se*
[b]*The ME/CFS Collaborative Research Centre at Uppsala University, Sweden*

† Electronic supplementary information (ESI) available. See DOI: https://doi.org/10.1039/d3ay01959d

This journal is © The Royal Society of Chemistry 2024

Open Access Article. Published on 29 January 2024. Downloaded on 5/21/2024 3:39:05 PM.
This article is licensed under a Creative Commons Attribution 3.0 Unported Licence.

energy metabolism through its downstream metabolites. This makes the pathway a crucial target for treatment.[2]

Tryptophan that escape hepatic degradation can traverse the blood–brain barrier and undergo hydroxylation, yielding 5-hydroxytryptophan which transforms into serotonin *via* decarboxylation catalyzed by aromatic L-amino acid decarboxylase.[12] Serotonin is best known as a key neurotransmitter responsible for regulating mood and producing melatonin, a hormone that helps control sleep patterns.[12] The indole pathway is a key part of tryptophan metabolism that involves the conversion of tryptophan into indole by gut bacteria. This produces substances like 3-hydroxy indole acetic acid, which has anti-inflammatory effects.[13]

The measurement of analytes beyond tryptophan metabolites is essential for gaining a comprehensive understanding of the complex biochemical pathways. For example, tyrosine and phenylalanine compete with tryptophan for transport across the blood–brain barrier. High levels of tyrosine and phenylalanine limit tryptophan's entry, decreasing its availability for serotonin synthesis. Measuring all three amino acid concentrations can thus help us assess metabolic competition.[14] Also, adequate levels of B-vitamins, such as riboflavin (B2) and pyridoxal phosphate (PLP), are crucial for their role as essential coenzymes in the metabolic process of tryptophan. Similarly, assessing the levels of hypoxanthine and neopterin can provide insights into oxidative stress and activation of the kynurenine pathway, which have been linked to inflammation and various diseases such as cancer and autoimmune disorders.[15]

Metabolomic analysis utilizes mass spectrometry techniques, often combined with chromatography, to effectively reduce sample complexity and minimize ion suppression. This study employed liquid chromatography and quadrupole Orbitrap tandem MS in parallel reaction monitoring (PRM) mode. Our method enables the simultaneous monitoring of multiple precursor and product ion transitions with high resolution and mass accuracy, offering flexibility in selecting fragment ion transitions after data acquisition.[16]

This study offers a solution to the challenges encountered in analyzing multiple analytes in human and murine tissue samples. These challenges arise from variations in the sample matrix, polarity, ionization effects, and endogenous levels, which hinder the full understanding of tryptophan metabolism. The current techniques are limited in their ability to measure only a small number of metabolites. For instance, a study conducted by Silva *et al.* utilized three different detection methods to examine eight tryptophan-related compounds in human and murine plasma.[17] This novel combination of analytes and unique application in the samples opens up new possibilities for a comprehensive understanding of tryptophan metabolism.

The aim of this research is to develop and validate a novel quantitative and semi-quantitative analytical method that utilizes liquid chromatography coupled to high resolution mass spectrometry (LC-HRMS) to accurately analyse more than 20 tryptophan metabolites and related compounds, as shown in the ESI Fig. S2,† in both human and murine tissue. The development of this method will facilitate future investigations into the relationship between these compounds and various physiological and pathological processes. Furthermore, it is of major importance to be able to compare results from animal models with clinical human samples, and thus facilitate further investigations of novel biomarkers and interventions. Our method is rapid with simple sample preparation, making it a valuable tool for investigating tryptophan metabolism across different species. However, some compounds did not meet the validation criteria and will require further adjustment.

2 Materials and methods

2.1 Chemicals

Purified deionized water with 18 MΩ cm conductivity was obtained using a Milli-Q water purification system (Millipore-Bedford, MA, USA). Whenever feasible, the analyte standards as shown in the ESI Table S1† were purchased from two different sources in order to allow independent preparation of calibration and quality control samples. Merck Life Science AB (Solna, Sweden) was the provider of the aforementioned standards except for quinolinic acid from Tocris Bioscience (Bristol, UK), dopamine hydrochloride and pantothenic acid calcium from the European Pharmacopoeia Reference Standard, serotonin and 5-hydroxytryptophan hydrochloride from Alfa Aesar, melatonin from Cayman Chemicals (Michigan, USA), and riboflavin from Supelco, while cyanocobalamin was sourced from Cerilliant. The vendor for stable isotope labeled internal standards as shown in the ESI Table S1† was Alsachim (Illkirch Graffenstaden, France), except for phenylalanine-[$^{2}H_5$], thiamine-[$^{13}C_3$], pyridoxine-[$^{2}H_3$], biotin-[$^{2}H_2$], folate-[$^{13}C_5$,^{15}N] and cyanocobalamin-[$^{13}C_7$] were purchased from Merck. Cambridge isotopes was the supplier of cystathionine-[$^{2}H_4$], tyrosine-[$^{2}H_7$], and dopamine-[$^{2}H_4$], while Supelco provided nicotinamide-[$^{13}C_6$]. Neopterin-[$^{13}C_5$] was acquired from Toronto Research Chemicals (Ontario, Canada) and serotonin-[$^{2}H_4$] hydrochloride from Cayman Chemicals. Lastly, methanol (LC/MS grade) and acetonitrile (LC/MS grade) were purchased from Fisher Scientific (Göteborg, Sweden), along with formic acid (LC/MS grade), ammonia solution 25%, and dimethyl sulfoxide (DMSO) from Merck Life Science AB (Solna, Sweden).

2.2 Calibration, quality controls and internal standard solutions

Standard stock solutions 1 mg mL^{-1} of picolinic acid, 3-hydroxyanthranilic acid, anthranilic acid, nicotinamide, phenylalanine, melatonin, serotonin, pantothenic acid, biotin, and cyanocobalamin were prepared in 100% methanol. Quinolinic acid, kynurenine, tryptophan, and 5-hydroxytryptophan were dissolved in a mixture of 50% acetonitrile and 50% water. 3-Hydroxykynurenine was prepared in a solution of 50% MeOH and 50% water with 0.1% formic acid. Xanthurenic acid, kynurenic acid, neopterin, and tyrosine were dissolved in 0.25 M NH_4OH. Pyridoxal 5′-phosphate, hypoxanthine, taurine, and cystathionine were dissolved in Milli-Q water. Dopamine-hydrochloride, riboflavin, and folate were dissolved in DMSO. These standard stock solutions were prepared in duplicate and

Open Access Article. Published on 29 January 2024. Downloaded on 5/21/2024 3:39:05 PM. This article is licensed under a Creative Commons Attribution 3.0 Unported Licence.

pooled into three groups (A, B and C) to create calibration and quality control solutions, as outlined in the ESI Table S2.† Stock solution A had the lowest concentration of the analyzed compounds, while stock B had an intermediate concentration; these two stocks were both diluted in methanol while stock C had the most concentrated level of analytes and was also diluted in methanol. Stock C was used for serial dilutions to prepare the calibration standards at eight different levels and quality control (QC) solutions at four levels; LLOQ, low, medium and high concentration levels for each targeted analyte as in the ESI Table S3.† Methanol was used for preparing all solutions. The final concentration for each analyte of the calibration and QC standards can be seen in the ESI Table S4.†

2.2.1 Preparation of stable isotope-labeled stock solutions (SILIS). Stock solutions 1 mg mL^{-1} of picolinic acid-[$^{2}H_4$], tryptophan-[$^{13}C_{11}$–$^{15}N_2$], anthranilic acid-[$^{13}C_6$], nicotinamide-[$^{13}C_6$], phenylalanine-[$^{2}H_5$], melatonin-[$^{2}H_4$], serotonin-[$^{2}H_4$] hydrochloride, theobromine, biotin-[$^{2}H_2$] were prepared in methanol. While, cyanocobalamin-[$^{13}C_7$] was purchased as a stock of 1 μg mL^{-1} in methanol. Quinolinic acid-[$^{13}C_4$,^{15}N], 3-hydroxykynurenine-[$^{13}C_6$], 3-hydroxyanthranilic acid-[$^{13}C_6$], neopterin-[$^{13}C_5$], dopamine-[$^{2}H_4$] hydrochloride and folate-[$^{13}C_5$,^{15}N] were dissolved in DMSO. Kynurenine-[$^{13}C_6$] and tryptophan-[$^{13}C_{11}$,$^{15}N_2$] were dissolved in 50% acetonitrile in water. Xanthurenic acid-[$^{13}C_6$], kynurenic acid-[$^{2}H_5$] and tyrosine-[$^{2}H_7$] were dissolved in 0.25 M NH_4OH. The internal standard (IS) working solution was created by combining the required concentration of the internal standard and adjusting the final volume with methanol, as outlined in the ESI Table S5.†

2.3 Biological samples

2.3.1 Human plasma. For this study, 24 presumed healthy donors (13 female, 11 male) with a mean age of 35 ± 15 years old provided plasma. All samples were collected between 9 and 11 a.m., following a 12 hour fast, except for three participants who were not fasting. Verbal and written consent were obtained from each donor, and the study was approved by the Ethical Review Agency (Dnr 2021-02859).

2.3.2 Murine samples. Left-over untreated control samples from a mouse model study conducted at Karolinska Institute (KI) was generously donated to our study by professor Jorge Ruas group. Twelve male HSA-Cre mice (1–2.5 months old) had been sacrificed by cervical dislocation and dissected for the collection of various samples. EDTA plasma, visceral and subcutaneous white adipose tissue were offered to our study. The samples were placed in individual Eppendorf tubes and stored at −80 °C for analysis. All animal experiments were conducted in accordance with local and international guidelines and approved by the local Ethics Committee.

2.4 Sample preparation

2.4.1 EDTA plasma. Human and murine plasma samples were thawed and vortexed briefly at 4 °C. An aliquot 75 μL of each sample, a calibration standard, a quality control and a blank were transferred to an Eppendorf tube followed by 25 μL of internal standard working solution as described in the ESI Table S5.† Protein precipitation was carried out by the addition of cold methanol 375 μL together with 25 μL of 0.1% formic acid. The mixture was vortexed for 15 seconds at 1600 rpm and kept at −20 °C for 30 minutes. Afterwards, the samples were centrifuged at 10 000 × *g* for 10 min at 4 °C and the supernatant 425 μL was collected and concentrated using nitrogen stream supplied by TurboVap (Biotage, Uppsala, Sweden) at the flow rate of 1.2 mL min^{-1} at 25 °C. After this, the dry residues were reconstituted in 100 μL of 0.1% formic acid in water and vortexed for 15 s at 1600 rpm. At last, the samples were centrifuged for 10 min at 10 000 × *g* at 4 °C to obtain the clear extract and the supernatant was transferred to amber LC vials for LC-HRMS analysis.

2.4.2 White adipose tissue. The frozen white adipose tissue from mice, both visceral and subcutaneous, was prepared similarly to plasma, with the exception of the weighing and homogenization steps. First, the tissue was weighed while still frozen, then transferred to an Eppendorf tube. Subsequently, 25 μL of internal standard working solution and 25 μL of 0.1% formic acid were added. Finally, 375 μL of cold methanol was added and the samples were homogenized in a FastPrep® (MP Biomedicals) at a speed of 6 m s^{-1} for 90 seconds.

2.5 LC-HRMS analysis

Analyses were conducted with a Waters Acquity UHPLC (Waters™) coupled to a high-resolution Q Exactive™ hybrid quadrupole-Orbitrap mass spectrometer (Thermo Scientific™). The LC column used was a Waters™ HSS T3 (1.8 μm: 2.1 × 100 mm) and the column oven temperature was set at 30 °C. The mobile phase consisted of Milli-Q water with 0.6% HCOOH (100 : 0.6%, v/v) (mobile phase A), and methanol with 0.6% HCOOH (100 : 0.6%, v/v) (mobile phase B) were delivered as a gradient at a flow rate of 300 μL min^{-1}, with a sample injection of 5 μL. The gradient was as follows: 1–10% B (0.0–4.0 min), 10–90% B (4.0–7.0 min), hold at 90% B (7.0–8.0 min), 90–1% B (8.0–8.1 min) followed by equilibration of the column at 1% B (8.1–9.0 min). The heated electrospray ionization (HESI) probe parameters were as follows: sheath gas flow rate, 40 units; auxiliary gas unit flow rate, 15 units; sweep gas flow rate, 2 units; capillary temperature, 360 °C; auxiliary gas heater temperature, 400 °C; spray voltage, 4.00 kV; and S lens, RF level 60. Parallel reaction monitoring (PRM) with an inclusion list, as seen in the ESI Table S1,† was utilized for mass spectrometry detection with a 1 *m*/*z* isolation window in positive electrospray ionization mode (ESI+) and acquired at a resolving power of 17 500 FWHM (full width half maximum) at *m*/*z* 200. The automatic gain control (AGC) was set at 2 × 10^5 and the injection time was set to 50 ms. Tune interface software (Tune v2.9, Thermo Scientific) was used for tuning and optimizing the analytes and Xcalibur® software (Version 4.1, Thermo Scientific) was used for data acquisition and processing by integrating selected product ion chromatographic peak area to calculate the metabolites concentration.

2.6 Method validation

The guidelines from the European Medicines Agency (EMA) on bioanalytical method validation were followed when carrying

 This journal is © The Royal Society of Chemistry 2024

Open Access Article. Published on 29 January 2024. Downloaded on 5/21/2024 3:39:05 PM. This article is licensed under a Creative Commons Attribution 3.0 Unported Licence.

out the method validation. This guideline was released on July 21, 2011 and is titled "Guideline on bioanalytical method validation EMEA/CHMP/EWP/192217/2009".

2.6.1 Linearity and lower limit of quantification (LLOQ). To assess linearity, calibration curves were prepared utilizing eight standard solutions made from methanol, as matrix-matched material was unavailable. The linearity range was determined by examining samples from six people and reported figures from the literature. The peak area response ratios (analyte peak area/IS peak area) were calculated and plotted against their corresponding nominal concentrations. Linear regression was employed, with $(1/X^2)$ used as a weighting factor. The linearity was deemed satisfactory if the regression factor was higher than 0.995. The lower limit of quantification was determined by preparing a separate standard solution at the same level of the first calibration point.

2.6.2 Accuracy and precision. Accuracy and precision of the analysis of QC samples at LLOQ, low, medium, and high concentration levels were determined to ensure the accuracy and reproducibility of the measurements. This was accomplished by calculating the % bias (calculated concentration − nominal concentration/nominal concentration) × 100 for accuracy estimation and the percent coefficient of variation (CV% = (standard deviation/mean) × 100) for precision. To ensure that the parameter levels of accuracy and precision between and within days were acceptable, 67% of all QCs (50% at each level) had to be within 15% (LLOQ 20%) of their nominal concentration.[18] This criterion was repeated on three independent days, with precision requirements of less than 20% for LLOQ and <15% for higher levels and accuracy requirements of within ±15% (up to 20% accepted for LLOQ).

2.6.3 Carry-over. In order to determine the analyte carry over, a solvent blank was injected three times after the highest calibration point on three consecutive days.

2.6.4 Matrix effect. The ionization efficiency of SILIS was evaluated by spiking it into human plasma samples after protein precipitation (six individuals × four replicates). In addition, SILIS was also spiked into a pure MeOH solution (six replicates). The matrix factor (MF) was calculated using the peak area of SILIS spiked into plasma divided by the peak area of SILIS spiked into the pure solution.

2.6.5 Recovery. To evaluate the accuracy of the extraction process of endogenous metabolites, SILIS were added to human plasma (six individuals × four replicates), and to the samples of visceral and subcutaneous white adipose tissue from six mice. The recovery was calculated by dividing the peak area of SILIS in the matrix after extraction by the peak area of SILIS in the matrix before extraction.

2.7 Semi-quantification analysis

A semi-quantitative analysis of six analytes was performed in human plasma ($n = 24$) and murine plasma ($n = 6$) to estimate their concentrations using an internal standard of close retention time. The formulae, RF = peak area/concentration and C suspect concentration = peak area suspect compound/RF similar compound,[19] were utilized to estimate the concentration of 3-indoleacetic acid using melatonin-[$^2H_4$] as IS, 5-hydroxyindoleacetic acid using kynurenine-[$^{13}C_6$]. Acetylcholine, asymmetric dimethylarginine and citrulline using thiamine-[$^{13}C_3$]. Lastly methionine using quinolinic acid-[$^{13}C_4$,^{15}N]. The mzCloud database was used for mass transitions selections and appropriate collision energies for the monitored parent ions as shown in the ESI Table S6.†

3 Results and discussion

Method development involved testing various solvents for protein precipitation, including methanol, methanol with water and 0.1% formic acid, and acetonitrile. Reconstitution solvents such as a mixture of methanol and water (1 : 9) and 0.1% formic acid in water were also compared. Our findings indicated that using methanol with 0.1% formic acid and reconstituting with 0.1% formic acid in water yielded slightly higher concentrations, although not significantly different from other solvent combinations. During our testing, we also encountered issues with double peaks for pyridoxine, pyridoxal phosphate, neopterin, hypoxanthine, and dopamine when using 0.1% formic acid in both mobile phases A and B. To address this problem, we increased the concentration of formic acid to 0.6% in both mobile phases A and B. This adjustment successfully resolved the issue and produced one peak in the chromatogram as shown in ESI Fig. S3.† Implementing high resolution in the measurement of complex samples, such as plasma and adipose tissue, is essential for accurate analysis and interpretation of results. The Orbitrap analyzer's high resolution allows for the separation of metabolite peaks in complex samples, reducing potential interferences and enhancing the accuracy of quantification. The LC-HRMS method developed in this study used retention times of precursor ions and at least one fragment ion to accurately measure metabolite levels as in the ESI Table S1.† The method was found to be effective in quickly analyzing 29 metabolites and estimate the concentration of six compounds in just 10 minutes. However, further adjustments are needed for some of the compounds as summarized in the ESI Table S7.†

3.1 Method validation

3.1.1 Linearity and low limit of quantification (LLOQ). The linearity of the calibration curves is presented in the ESI Table S8† and the low limit of quantification (LLOQ) values are summarized in the ESI Table S4.† Each calibration curve consisted of a minimum of five calibration points and most of the analytes showed a correlation coefficient > 0.99, with the exception of 3-hydroxykynurenine, anthranilic acid, xanthurenic acid, kynurenic acid, biotin, nicotinamide, neopterin, cystathionine, 5-hydroxytryptophan, pyridoxal 5′-phosphate, and hypoxanthine. This could be attributed to the possibility that these analytes were eluted at the same time, or that there were issues with their solubility during the experiment. The lowest correlation coefficient was 0.944 for neopterin. The LLOQ ranged from 1 to 200 ng mL^{-1}, with the lowest LLOQ of 1 ng mL^{-1} obtained for pyridoxine. Some compounds prepared at

Open Access Article. Published on 29 January 2024. Downloaded on 5/21/2024 3:39:05 PM. This article is licensed under a Creative Commons Attribution 3.0 Unported Licence.

LLOQ lower than 1 ng mL^{-1} did not meet the validation criteria and were not included in the analysis.

3.1.2 Accuracy and precision. The results of the intra- and interday precision and accuracy of the assay are presented in the ESI Table S9.† In total nine out of 22 analytes passed both the intra- and interday precision and accuracy criteria for 67% of QCs (50% at each level) were within 15% (LLOQ 20%). The nine analytes were: hydroxyanthranilic acid, hydroxykynurenine, hydroxytryptophan, kynurenine, pantothenic acid, phenylalanine, pyridoxine, tryptophan and tyrosine. Other nine analytes out of the 22 passed the intra-and interday precision and accuracy at different QC's levels as shown next: cystathionine passed at LLOQ, QCM and QCH. Riboflavin passed at QCL, QCM and QCH. Biotin, hypoxanthine, nicotinamide and quinolinic acid passed at QCM and QCH. Xanthurenic acid passed at QCL and QCM. Kynurenic acid and serotonin passed only at QCL. The rest four analytes out of the 22 did not pass the intra- nor the interday precision and accuracy criteria at any QC's level. Those compounds were: anthranilic acid, melatonin, neopterin and pyridoxal phosphate. The interday precision determinations represented by CV (%) ranged from 0.001% for phenylalanine at LLOQ level to 12.7% for pyridoxal phosphate at LLOQ level. The interday accuracy determinations represented by bias (%) ranged from 0.004% for hypoxanthine at QCH to 11.2% for cystathionine at QCH.

3.1.3 Carry-over. All target metabolites demonstrated minimal carryover (<10%) for most metabolites except for; nicotinamide, xanthurenic acid and anthranilic acid that showed carry-over criteria (>15%).

3.1.4 Matrix effect. A barplot was produced as shown in ESI Fig. S4† to illustrate the level of ion suppression/enhancement of each SILIS from human plasma (6 individuals × 4 replicates), murine subcutaneous and visceral white adipose tissue ($n = 6$ for each). The mean matrix factor ranged from 2.2%, 13.4%, and 15.4% for cystathionine-[$^2H_4$] in plasma, murine subcutaneous and visceral white adipose tissue, respectively, which was found to be suppressed due to elution at the dead time, to 164.6%, 173.8%, and 268.3% for serotonin-[$^2H_4$], serotonin-[$^2H_4$], and theobromine, in plasma, murine subcutaneous, and visceral white adipose tissue, respectively, which were found to be enhanced. Error bars indicating the CV% for each SILIS were included, with all values lower than 15%, except for tyrosine-[$^2H_7$] (24%) and theobromine (44%) in plasma, cystathionine-[$^2H_4$] (27.2%) in subcutaneous white adipose tissue, 3-hydroxykynurenine-[$^{13}C_6$] (15.1%) and serotonin-[$^2H_4$] (46.6%) in visceral white adipose tissue.

3.1.5 Recovery. The evaluation of 18 SILIS in human plasma as shown in ESI Fig. S5† revealed that their mean recoveries ranged from 50% (tyrosine-[$^2H_7$]) to 141% (serotonin-[$^2H_4$]) with all recoveries above 100%, except for tyrosine-[$^2H_7$] and theobromine (50% and 99% respectively). A low plasma recovery was also reported by J. Marcos *et al.*, which reported a recovery of 72% for tyrosine in plasma.[20] Most had a CV% of less than 15%, except for cystathionine-[$^2H_4$] (31%). In murine visceral white adipose tissue, the mean recoveries ranged from 41% (tyrosine-[$^2H_7$]) to 267% (quinolinic acid-[$^{13}C_4$,^{15}N]), with all recoveries above 100%, except for tyrosine-[$^2H_7$], biotin-[$^2H_2$], serotonin-[$^2H_4$], pyridoxine-[$^2H_3$] and phenylalanine-[$^2H_5$] (41%, 87%, 97%, 99%, 99% respectively). Most had a CV% of less than 15%, except for nicotinamide-[$^{13}C_6$], tyrosine-[$^2H_7$], quinolinic acid-[$^{13}C_4$,^{15}N], biotin-[$^2H_2$], melatonin-[$^2H_4$] and anthranilic acid-[$^{13}C_6$] (15%, 19%, 21%, 21%, 31%, 58% respectively). In murine subcutaneous white adipose tissue, the mean recoveries ranged from 47% (tyrosine-[$^2H_7$]) to 186% (neopterin-[$^{13}C_5$]), with all recoveries above 100%, except for tyrosine-[$^2H_7$], serotonin-[$^2H_4$], biotin-[$^2H_2$], phenylalanine-[$^2H_5$] and kynurenic acid-[$^2H_5$] (47%, 77%, 90%, 93%, 96% respectively). Most had a CV% of less than 15%, except for 3-hydroxykynurenine-[$^{13}C_6$], phenylalanine-[$^2H_5$], kynurenic acid-[$^2H_5$], cystathionine-[$^2H_4$], nicotinamide-[$^{13}C_6$], pyridoxine-[$^2H_3$], quinolinic acid-[$^{13}C_4$,^{15}N], tryptophan-[$^{13}C_{11}$,$^{15}N_2$], xanthurenic acid-[$^{13}C_6$] and neopterin-[$^{13}C_5$] (15%, 16%, 16%, 16%, 18%, 20%, 22%, 22%, 26%, 33% respectively).

3.2 Application of the method to biological samples

3.2.1 Quantitative analysis of murine samples. Tryptophan has been shown to affect adipogenesis, fat storage, thermogenesis and other metabolic processes so analysis of tryptophan metabolites can help to identify biochemical pathways associated with obesity and diabetes.[21] Subcutaneous and visceral white adipose tissues are known to have distinct metabolic roles *e.g.* a build-up of visceral adipose tissues is associated with insulin resistance and metabolic diseases, whereas excess accumulation of subcutaneous adipose tissues is thought to be protective.[22] A study of Ogura *et al.* suggests that tryptophan, phenylalanine, tyrosine and serotonin are present at higher concentrations in subcutaneous adipose tissue than in visceral white adipose tissue.[23] This finding was confirmed in the current study as shown in ESI Fig. S6,† though the level of phenylalanine exceeded the linear range of our method and was thus excluded from the calculation since the method had not been validated for dilution integrity.

Comparative analysis of murine and human plasma revealed that the concentrations of most of the compounds quantified were higher in murine plasma as shown in Fig. 1, except for kynurenine and quinolinic acid, with the median concentration of most analytes in murine plasma ranging from 4 ng mL^{-1} (biotin) to 16 020 ng mL^{-1} (tryptophan). The comparison of tryptophan metabolites in mice and humans revealed an opposite trend; the levels of plasma serotonin in mice were found to be higher than those of kynurenine, whereas the opposite was observed in humans. This disparity can be attributed to the varying tryptophan metabolism and enzyme activities in the kynurenine pathway among different species, particularly in the central nervous system. For example, rats have lower IDO1 induction in response to immune stimulation compared to mice, while gerbils are more similar to humans in their increase of quinolinic acid levels during inflammation.[24] These differences revealed the necessity to select the right species when studying the physiological and pathological effects of kynurenine pathway activity.

In our study, we measured the levels of (phenylalanine, pantothenic acid, tyrosine, 3-hydroxyanthranilic acid,

 This journal is © The Royal Society of Chemistry 2024

Open Access Article. Published on 29 January 2024. Downloaded on 5/21/2024 3:39:05 PM.
This article is licensed under a Creative Commons Attribution 3.0 Unported Licence.

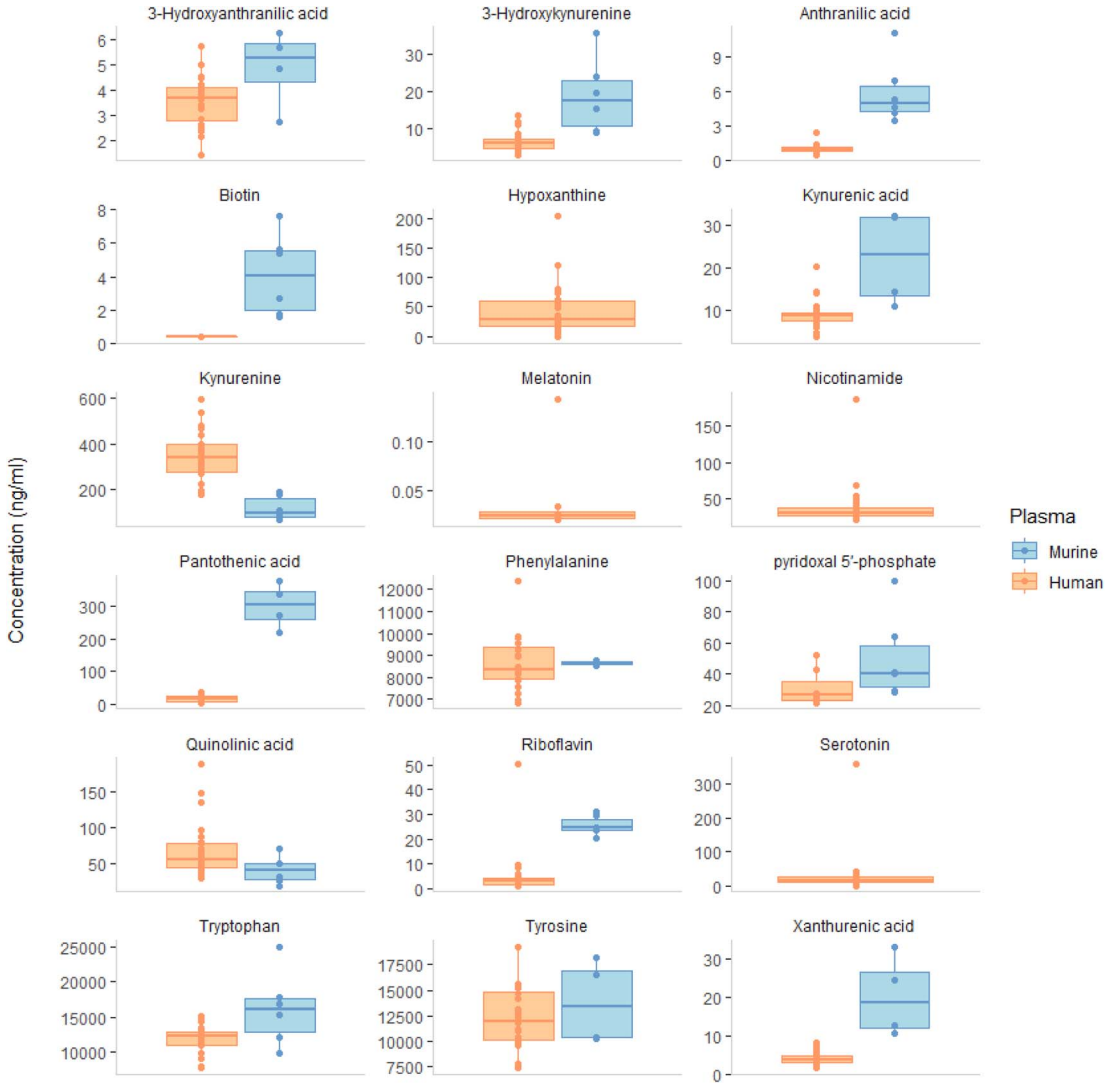

Fig. 1 The median concentrations of the aromatic amino acids; tryptophan and its metabolites, tyrosine and phenylalanine. In addition to B vitamins (biotin, pantothenic acid, pyridoxal 5′-phosphate and riboflavin) and the oxidation marker hypoxanthine were determined in ng mL^{-1} in human ($n = 24$) and murine ($n = 6$) plasma from healthy controls. Comparing the concentration of analytes in murine and human plasma, the results showed that most compounds were higher in murine plasma. The only two exceptions were kynurenine and quinolinic acid. The analyte concentration in murine plasma ranged from 4 ng mL^{-1} (biotin) to 16 020 ng mL^{-1} (tryptophan). Nicotinamide and serotonin had median values above ULOQ, while melatonin and hypoxanthine were not detected and thus omitted from the boxplot results.

kynurenic acid, and xanthurenic acid). The median concentrations of these analytes ranged from 5 to 8675 ng mL^{-1}, with some values exceeding the upper limit of quantification (ULOQ) and thus being excluded from the calculation with the exception of 3-hydroxyanthranilic acid, which fell below LLOQ. Nicotinamide and serotonin had median values above ULOQ, while melatonin and hypoxanthine, were not detected and therefore excluded from the boxplot results. Our observed high levels of murine serotonin are consistent with previous research by Rubio *et al.*[25]

3.2.2 Quantitative analysis of human samples. Comparing the results of our study to other published findings was rather tedious since various factors, such as sample source (plasma or serum), fasting status, sample preparation and analytical methods, as well as demographic information of the control group can introduce a degree of variance and make comparison challenging. To further illustrate the results of our study, values were plotted in relation to other published LC-MS and LC-fluorescence methods, as seen in ESI Fig. S7.† The analysis of 24 human plasma samples revealed that biotin, riboflavin and 3-hydroxy anthranilic acid had the lowest concentrations (0.35, 3.01 and 3.71 ng mL^{-1}), respectively. While tryptophan, tyrosine, and phenylalanine had the highest concentrations (12 221, 11 985, and 8361 ng mL^{-1}), respectively. Our study found that biotin levels were much lower than another study with an average of 22.8 ng mL^{-1} for 2 out of 20 participants.[26] Our riboflavin result of 3.01 ng mL^{-1} was similar to those reported from 4–9 ng mL^{-1}.[26–28] Moreover, our result for 3-hydroxy anthranilic acid concentration was 5.2 ng mL^{-1}, which was consistent with a study conducted using Q-Exactive method in

Open Access Article. Published on 29 January 2024. Downloaded on 5/21/2024 3:39:05 PM.
This article is licensed under a Creative Commons Attribution 3.0 Unported Licence.

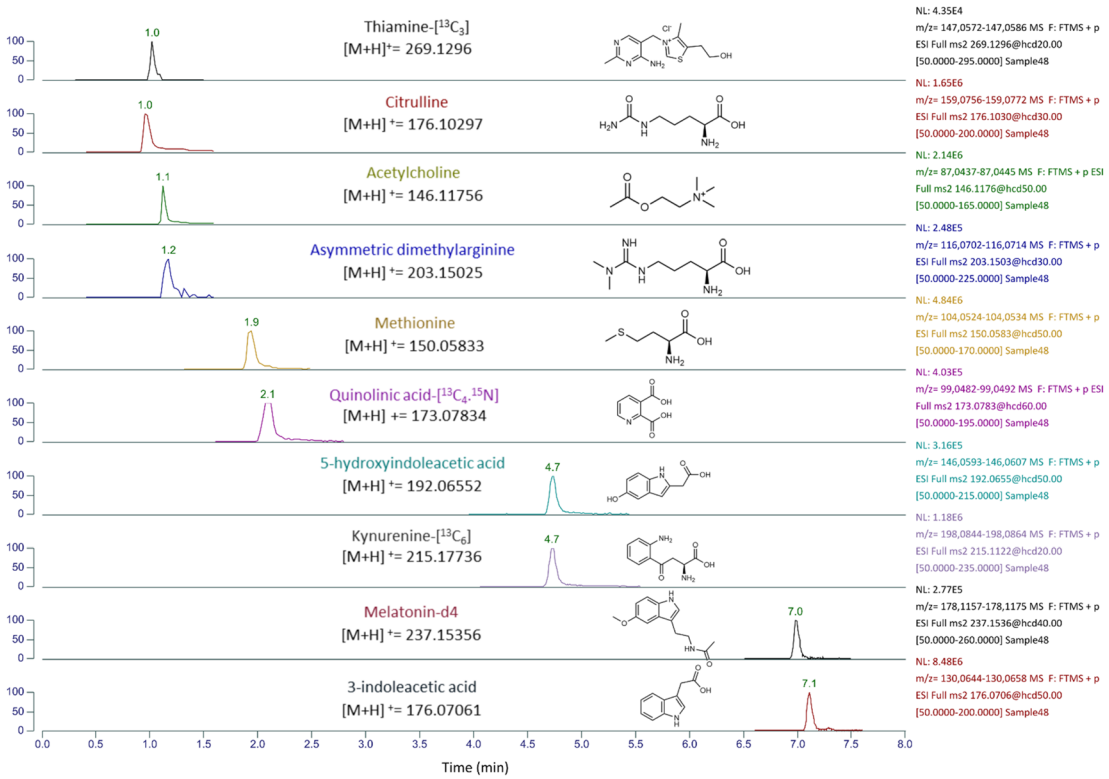

Fig. 2 An extracted ion chromatogram, of the semi quantification analysis, was generated for thiamine-[$^{13}C_3$] which was used as an internal standard (IS) to estimate the concentrations of citrulline, acetylcholine, and asymmetric dimethylarginine, which all elute at a similar retention time (RF similar compound). Additionally, quinolinic acid-[$^{13}C_4$,^{15}N] was used as an IS for methionine, kynurenine-[$^{13}C_6$] as an IS for 5-hydroxyindoleacetic acid, and melatonin-[$^{2}H_4$] as an IS for 3-indoleacetic acid. The concentration estimation of these analytes was performed using the equations: $\mathrm{RF} = \frac{\text{peak area}}{\text{concentration}}$ and C suspect concentration $= \frac{\text{peak area of suspect compound}}{\text{RF similar compound}}$.

214 healthy control subjects.[29] The levels of tryptophan and tyrosine in our study were comparable to those found in other studies[18,27,29–34] as displayed in ESI Fig. S8.† Tryptophan, tyrosine and phenylalanine, are used to produce neurotransmitters such as serotonin, dopamine, norepinephrine and GABA which contribute to physical and emotional wellbeing.[34] Regarding the serotonin pathway, our method wasn't sensitive enough to measure melatonin and matrix effect might hinder the detection of 5 hydroxytryptophan in plasma. According to other studies, 5 hydroxytryptophan was found ranging from 0.9 to 10.9 ng mL^{-1} (ref. 29–34) and melatonin was found at 0.007 ng mL^{-1} with 102 participants.[35] Our value for serotonin 17.1 ng mL^{-1} was within the 1.8–103 ng mL^{-1} range reported in other studies.[34,36] Ultimately, it appears that using platelets are a superior marker of serotonin levels than plasma, as they reflect long-term serotonin activity and are not impacted by dietary intake. Siliconized glassware and plastic ware should be used to improve accuracy in serotonin measurement.[37]

A range of tryptophan metabolites reported from previous studies included anthranilic acid 0.5–13.4 ng mL^{-1},[29,32] 3 hydroxyanthranilic acid 3.2–10.7 ng mL^{-1},[32,36] kynurenic acid 1.9–14 ng mL^{-1},[32,36] 3-hydroxykynurenine 1.9–47 ng mL^{-1},[18,36] xanthurenic acid 1.2–68.1 ng mL^{-1},[29,38] nicotinamide 21.1–147.3 ng mL^{-1},[26,39] quinolinic acid 39–180 ng mL^{-1},[36,38] kynurenine 43.7–1790 ng mL^{-1},[34,36] and picolinic acid 3.2–49.4 ng mL^{-1}.[29,33] Using our method, it was observed that the isomers picolinic acid and niacin were unable to be differentiated through chromatography. Others have achieved to separate those compounds through the addition of 0.5% formic acid and 1 mM ammonium formate.[36]

3.2.3 Semi quantitative analysis. Semi-quantitative analysis is a cost-effective way to assess the relative abundance of metabolites in a sample, as it is less time-consuming and more affordable than full quantitative methods. To assess six analytes in human plasma ($n = 24$) and murine plasma ($n = 6$), our semi-quantitative method was used as an initial step as shown in Fig. 2, and the results of human plasma as plotted in the ESI Fig. S9,† were then compared to those from other studies that used quantitative methods. Comparative studies, however, were not available for murine plasma. For 5-hydroxyindoleacetic acid and 3-indoleacetic acid, our method measured a concentration of 62.8 and 100.8 ng mL^{-1} respectively, compared to 7.8 and 181.6 ng mL; $n = 100$, reported by Chen *et al.*[32] We reported a higher concentration of citrulline (8827.7 ng mL^{-1} compared to 6562.5 ng mL; $n = 15$),[40] asymmetric dimethylarginine (1102.6 compared to 135.5 ng mL; $n = 15$),[40] acetylcholine (4973.2 ng mL^{-1} compared to 0.456 ng mL; $n = 30$),[41] and methionine (4143.3 compared to 3605.8 ng mL^{-1}; $n = 13$).[42] Our results for acetylcholine were particularly high compared to those of other studies, suggesting that an alternative internal standard should

 This journal is © The Royal Society of Chemistry 2024

Open Access Article. Published on 29 January 2024. Downloaded on 5/21/2024 3:39:05 PM.
This article is licensed under a Creative Commons Attribution 3.0 Unported Licence.

be evaluated or that an external calibration curve should be used for quantitative results. Overall, our semi-quantitative results for 3-indoleacetic acid, methionine and citrulline were comparable to those of other studies; nevertheless, caution is advised when interpreting concentrations measured using semi-quantitative methods. Those analytes can however be used for the assessment of *e.g.* gastrointestinal functions.

There are several potential explanations for why certain analytes may have failed to pass in the study. One possible reason could be the instability of these analytes to various environmental factors, such as light, heat, and acidity. For example, compounds like folic acid and cyanocobalamin may be prone to degradation in these conditions. Additionally, the combined effects of low ionization efficiency, matrix effects, and low concentration may have made it difficult to accurately detect and quantify other compounds listed in the ESI Table S7.† In order to address these issues, it is important to continue developing and exploring alternative LC gradient and sample preparation methods to mitigate the likelihood of analyte degradation.

4 Conclusions

In this study we present a fast and simple methodology for the investigation of tryptophan metabolism, applied in human plasma as well as murine plasma and adipose tissue. We want to highlight the importance of understanding the differences in tryptophan metabolism among species and tissues, as well as the need to consider species-specific differences when studying human pathological conditions as compared with animal models. Also, we provide valuable data for the need of future developments of standardized methodologies for accurate quantification of tryptophan metabolites and B vitamins. This study reveals that tryptophan metabolites vary widely across studies and can be influenced by different factors such as study population, sample preparation and types of analyzers used. Our high resolution mass spectrometric method for quantifying tryptophan metabolites and B vitamins in human and murine tissues offers a practical and effective option for use in clinical settings. In addition, our semi-quantitative technique allows for accurate identification of metabolites in a sample, with results similar to quantitative methods for some analytes.

Author contributions

SA, KU, and JB designed the study. SA performed the experimental work. SA analysed the data. SA wrote the manuscript drafts. All authors revised and approved the final version of the manuscript.

Conflicts of interest

There are no conflicts to declare.

Acknowledgements

Open Medicine Foundation is acknowledged for the kind support of this study. We thank Bhagya Kolitha for his assistance in sample preparation, and also extend our thanks to Sooraj Baijnath and Juan R. Lopez-Edigo for their valuable input and review of our manuscript.

References

1 S. Khemaissa, S. Sagan and A. Walrant, *Crystals*, 2021, **11**(9), DOI: **10.3390/cryst11091032**.
2 S. Taleb, *Front. Immunol.*, 2019, **10**, 1–7.
3 T. V. Lanz, S. K. Williams, A. Stojic, S. Iwantscheff, J. K. Sonner, C. Grabitz, S. Becker, L. I. Böhler, S. R. Mohapatra, F. Sahm, G. Küblbeck, T. Nakamura, H. Funakoshi, C. A. Opitz, W. Wick, R. Diem and M. Platten, *Sci. Rep.*, 2017, **7**, 1–13.
4 M. Kanai, H. Funakoshi, H. Takahashi, T. Hayakawa, S. Mizuno, K. Matsumoto and T. Nakamura, *Mol. Brain*, 2009, **2**, 1–16.
5 R. Zulpaite, P. Miknevicius, B. Leber, K. Strupas, P. Stiegler and P. Schemmer, *Int. J. Mol. Sci.*, 2021, **22**, 1–32.
6 A. A. B. Badawy, *Int. J. Tryptophan Res.*, 2017, **10**, DOI: **10.1177/1178646917691938**.
7 S. Kim, B. J. Miller, M. E. Stefanek and A. H. Miller, *Cancer*, 2015, **121**, 2129–2136.
8 J. Savitz, *Mol. Psychiatry*, 2020, **25**, 131–147.
9 M. Cespedes, K. R. Jacobs, P. Maruff, A. Rembach, C. J. Fowler, B. Trounson, K. K. Pertile, R. L. Rumble, S. R. Rainey-Smithe, C. C. Rowe, V. L. Villemagne, P. Bourgeat, C. K. Lim, P. Chatterjee, R. N. Martins, A. Ittner, C. L. Masters, J. D. Doecke, G. J. Guillemin and D. B. Lovejoy, *Neurobiol. Dis.*, 2022, **171**, 105783.
10 C. K. Lim, F. J. Fernández-Gomez, N. Braidy, C. Estrada, C. Costa, S. Costa, A. Bessede, E. Fernandez-Villalba, A. Zinger, M. T. Herrero and G. J. Guillemin, *Prog. Neurobiol.*, 2017, **155**, 76–95.
11 W. Marx, A. J. McGuinness, T. Rocks, A. Ruusunen, J. Cleminson, A. J. Walker, S. Gomes-da-Costa, M. Lane, M. Sanches, A. P. Diaz, P. T. Tseng, P. Y. Lin, M. Berk, G. Clarke, A. O'Neil, F. Jacka, B. Stubbs, A. F. Carvalho, J. Quevedo, J. C. Soares and B. S. Fernandes, *Mol. Psychiatry*, 2021, **26**, 4158–4178.
12 E. Höglund, Ø. Øverli and S. Winberg, *Front. Endocrinol.*, 2019, DOI: **10.3389/fendo.2019.00158**.
13 H. Ormstad, C. S. Simonsen, L. Broch, D. M. Maes, G. Anderson and E. G. Celius, *Mult. Scler. Relat. Disord.*, 2020, **46**, 102533.
14 H. Barone, Y. T. Bliksrud, I. B. Elgen, P. D. Szigetvari, R. Kleppe, S. Ghorbani, E. V. Hansen and J. Haavik, *Am. J. Med. Genet., Part B*, 2020, **183**, 95–105.
15 R. Fuertig, A. Ceci, S. M. Camus, E. Bezard, A. H. Luippold and B. Hengerer, *Bioanalysis*, 2016, **8**, 1903–1917.
16 J. Zhou, H. Liu, Y. Liu, J. Liu, X. Zhao and Y. Yin, *Anal. Chem.*, 2016, **88**, 4478–4486.
17 P. Valente-Silva, I. Cervenka, D. M. S. Ferreira, J. C. Correia, S. Edman, O. Horwath, B. Heng, S. Chow, K. R. Jacobs, G. J. Guillemin, E. Blomstrand and J. L. Ruas, *Metabolites*, 2021, **11**(8), DOI: **10.3390/metabo11080508**.

Open Access Article. Published on 29 January 2024. Downloaded on 5/21/2024 3:39:05 PM. This article is licensed under a Creative Commons Attribution 3.0 Unported Licence.

18 L. Whiley, L. C. Nye, I. Grant, N. Andreas, K. E. Chappell, M. H. Sarafian, R. Misra, R. S. Plumb, M. R. Lewis, J. K. Nicholson, E. Holmes, J. R. Swann and I. D. Wilson, *Anal. Chem.*, 2019, **91**, 5207–5216.
19 L. Malm, E. Palm, A. Souihi, M. Plassmann, J. Liigand and A. Kruve, *Molecules*, 2021, **26**, 3524.
20 J. Marcos, N. Renau, O. Valverde, G. Aznar-Laín, I. Gracia-Rubio, M. Gonzalez-Sepulveda, L. A. Pérez-Jurado, R. Ventura, J. Segura and O. J. Pozo, *J. Chromatogr. A*, 2016, **1434**, 91–101.
21 W. Hu, G. Yan, Q. Ding, J. Cai, Z. Zhang, Z. Zhao, H. Lei and Y. Z. Zhu, *Biomed. Pharmacother.*, 2022, **150**, 112957.
22 Q. Luong, J. Huang and K. Y. Lee, *Biology*, 2019, **8**, 1–14.
23 Y. Okamatsu-Ogura, M. Kuroda, R. Tsutsumi, A. Tsubota, M. Saito, K. Kimura and H. Sakaue, *Metabolism*, 2020, **113**, 154396.
24 Y. Murakami and K. Saito, *Int. J. Tryptophan Res.*, 2013, **6**, 47–54.
25 V. Y. Rubio, J. G. Cagmat, G. P. Wang, R. A. Yost and T. J. Garrett, *Anal. Chem.*, 2020, **92**, 2550–2557.
26 K. Meisser Redeuil, K. Longet, S. Bénet, C. Munari and E. Campos-Giménez, *J. Chromatogr. A*, 2015, **1422**, 89–98.
27 O. Midttun, S. Hustad and P. M. Ueland, *Rapid Commun. Mass Spectrom.*, 2009, **23**, 1371–1379.
28 P. Chen, Y. Tang, Q. He, L. Liu, Z. Zhou, Y. Song, N. Zhang, B. Wang, H. Zhou, H. Shi and J. Jiang, *J. Pharm. Biomed. Anal.*, 2022, **219**, 114944.
29 R. Colle, P. Masson, C. Verstuyft, B. Fève, E. Werner, C. Boursier-Neyret, B. Walther, D. J. David, B. Boniface, B. Falissard, P. Chanson, E. Corruble and L. Becquemont, *Psychiatry Clin. Neurosci.*, 2020, **74**(2), 112–117.
30 B. A. Acids, A. Anesi, K. Berding, G. Clarke, C. Stanton, J. F. Cryan, N. Caplice, R. P. Ross, A. Doolan, U. Vrhovsek and F. Mattivi, *J. Proteome Res.*, 2022, **21**(5), 1262–1275.
31 K. M. Ryan, K. A. Allers, D. M. McLoughlin and A. Harkin, *Brain, Behav., Immun.*, 2020, **83**, 153–162.
32 K. H. Chang, M. L. Cheng, H. Y. Tang, C. Y. Huang, Y. R. Wu and C. M. Chen, *Mol. Neurobiol.*, 2018, **55**, 6319–6328.
33 S. Adams, C. Teo, K. L. McDonald, A. Zinger, S. Bustamante, C. K. Lim, G. Sundaram, N. Braidy, B. J. Brew and G. J. Guillemin, *PLoS One*, 2014, **9**, 1–28.
34 S. C. James, K. Fraser, J. Cooney, C. S. Günther, W. Young, R. B. Gearry, P. E. Heenan, T. Trower, J. I. Keenan, N. J. Talley, W. C. McNabb and N. C. Roy, *Metabolites*, 2023, **13**, DOI: **10.3390/metabo13020313**.
35 P. J. Eugster, M. Dunand, B. Grund, A. Ivanyuk, N. Fogarasi Szabo, C. Bardinet, K. Abid, T. Buclin, E. Grouzmann and H. Chtioui, *Clin. Chim. Acta*, 2022, **535**, 19–26.
36 A. Anesi, K. Berding, G. Clarke, C. Stanton, J. F. Cryan, N. Caplice, R. P. Ross, A. Doolan, U. Vrhovsek and F. Mattivi, *J. Proteome Res.*, 2022, **21**(5), 1262–1275.
37 T. Audhya, J. B. Adams and L. Johansen, *Biochim. Biophys. Acta, Gen. Subj.*, 2012, **1820**, 1496–1501.
38 A. Desmons, L. Humbert, T. Eguether, P. Krasniqi, D. Rainteau, T. Mahdi, N. Kapel and A. Lamazière, *J. Chromatogr. A*, 2022, **1685**, 463602.
39 G. R. Ibrahim, I. Shah, S. Gariballa, J. Yasin, J. Barker and S. S. Ashraf, *Molecules*, 2020, **25**, DOI: **10.3390/molecules25173932**.
40 J. Martens-Lobenhoffer and S. M. Bode-Böger, *J. Chromatogr. B: Anal. Technol. Biomed. Life Sci.*, 2003, **798**, 231–239.
41 K. Kawashima, T. Fujii, Y. Moriwaki and H. Misawa, *Life Sci.*, 2012, **91**, 1027–1032.
42 O. Galilea San Blas, F. Moreno Sanz, P. Herrero Espílez, B. Prieto García, F. V. Álvarez Menéndez, J. M. Marchante-Gayón and J. I. García Alonso, *J. Anal. At. Spectrom.*, 2016, **31**, 1885–1894.

This journal is © The Royal Society of Chemistry 2024